Interaction Notes

Note 608

February 2009

LIGHTNING INDUCED WAVEFORM 5 IN COMPOSITE AIRFRAMES, THE INABILITY OF COPPER BRAID TO SHIELD IT, AND A NEW LAYERED COPPER BRAID AND HIGH-MU FOIL SHIELD

Larry West
10215 Beechnut St., Suite 1003
Houston, TX 77072

Abstract

A simple theory is presented of how lightning induced Waveform 5 currents appears on cables in composite airframes and why it does not rise as fast as the lightning pulse or as slow as the RL time constant of the cable. Why normal copper braid shields do not work against it is explained using Schelkunoff's theory of coaxial cable shields. A new cable shield design using layers of copper and high-mu foil is developed that will protect against Waveform 5 currents and not saturate. The effects of the new cable shield on signals passing through it are discussed. Finally, a lab test is designed for verifying the models.

INTRODUCTION

This paper is possibly the first open publication of (1) a simple theory of how the low frequency Waveform 5 induced lightning current (44-50μs rise time and 100-500μs decay time)[4] develops on cables in composite airframes, (2) why normal copper braid cable shields do not attenuate the low frequencies, and (3) a new cable shield design[21] for protecting electrical and electronic systems from this little understood phenomenon. More rigorous theoretical work is needed.

Composite airframes exposed to direct strike lightning with as much as 200kA current will have over ten thousand volts built up along the airframe. A notional picture of a composite cylindrical airframe with a shielded wire is shown in Figure 1. A 1kΩ source impedance would be acceptable to the phenomenologists but it is unnecessary for this modeling because it is much larger than the loads.

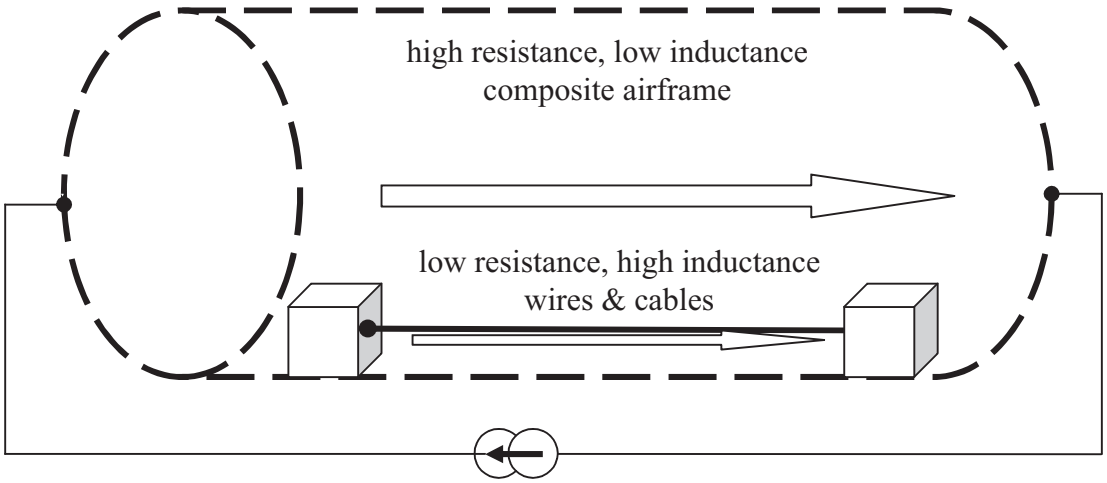

Figure 1 Composite Airframe with Shielded Cable/Wire

The composite skin has high resistance and low inductance while the metallic interior wiring and plumbing have relatively lower resistance and higher inductance. The division of the lightning current between the two and the voltage across the two defines the induced environment for avionics.

The problem is exacerbated when the skin depth is equal to or greater than the braid shield thickness and the separation of the internal and shielded internal regions governed by their separate boundary conditions loosely coupled by a small transfer impedance and admittance disappears.

This note treats the latter problem of induced currents on the cable shields so low in frequency that the skin depth is greater than the copper cable shield thickness using Schelkunoff's 74 year old theory.[1] A new cable shield design is then developed using layers of copper braid and high-mu foil. Note that throughout, the boxes' shield thickness is assumed to be large compared to that of the cable shield and the box's skin depth.

The author would like to thank the following people for many conversations about this elusive little investigated subject that affects every composite vehicle: J. A. (Andy) Plumer, Tom Pierce, Roxanne Arellano, Jim Lambert, Bob Scully, and Carl E. Baum.

SIMPLE LOW FREQUENCY CIRCUIT MODEL FOR CURRENT DIVISION

A simple circuit model of Figure 1 follows:

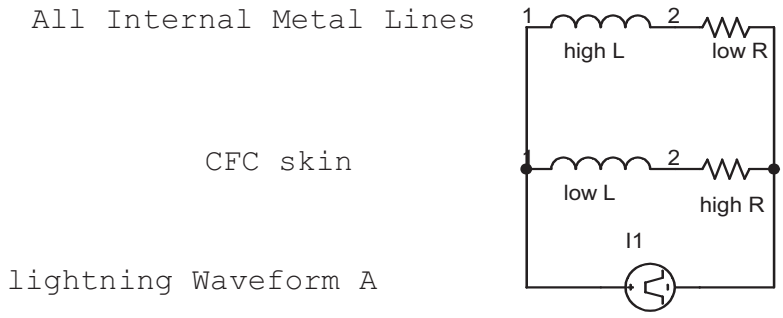

Figure 2 Simple Circuit Model for Lightning Current Distribution in a Composite Airframe

As a notional example, we will use a 100mΩ, 500nH, composite skin and a 20mΩ, 3μH, internal braid. The driving current is the SAE ARP5412A Waveform A[4] with a rise time of $(647{,}245)^{-1}$ sec, a fall time of $(11{,}354)^{-1}$ sec, and a peak amplitude of 200kA for the double exponential.

The lightning Waveform A is as follows in the time domain:

$$I(t) = I_0 \cdot \left(e^{-a \cdot t} - e^{-b \cdot t}\right) \cdot u(t) \tag{1}$$

where

b = 647,265 sec^{-1} = 1/1.5μs,
a = 11,354 sec^{-1} = 1/88μs,
I_0 is 218,810 amps, which gives the peak double exponential amplitude of 200kA, and
u(t) = unit step function.

The Laplace transform of the lightning waveform is as follows:

$$\widetilde{I}(s) = \frac{I_0}{s} \cdot \left(\frac{1}{s+a} - \frac{1}{s+b} \right). \tag{2}$$

The voltage across the system is as follows:

$$\widetilde{V}(s) = \widetilde{I}(s) \cdot \widetilde{Z}(s) \tag{3}$$

where $Z(s)$ is impedance of the two parallel branches:

$$\widetilde{Z}(s) = \left(\frac{1}{R_{CFC} + s \cdot L_{CFC}} + \frac{1}{R_{braid} + s \cdot L_{braid}} \right)^{-1} = \frac{L_{CFC} \cdot L_{braid}}{L_{CFC} + L_{braid}} \cdot \frac{(s+\alpha) \cdot (s+\beta)}{s+\gamma} \tag{4}$$

where

L_{braid} is the braid inductance, 3μH,
L_{CFC} is the composite (CFC) skin inductance, 500nH,
R_{braid} = 20mΩ
R_{CFC} = 100mΩ
$\alpha = R_{braid}/L_{braid}$ = 1/150μs,
$\beta = R_{CFC}/L_{CFC}$ = 1/5μs,
$\gamma = (R_{braid}+R_{CFC})/(L_{braid}+L_{CFC})$ = 1/29μs, the loop inverse time constant.

For the example, above, the induced voltage across the airframe is shown in Figure 3, below, along with Waveform 4 normalized to the same peak. We have tacitly assumed that the voltage across the airframe is the lightning Waveforms A, 1, & 4 which it is not because the impedance is not resistive. Note that all of the time domain graphs use logarithmic scale in time in order to accentuate the early time effects.

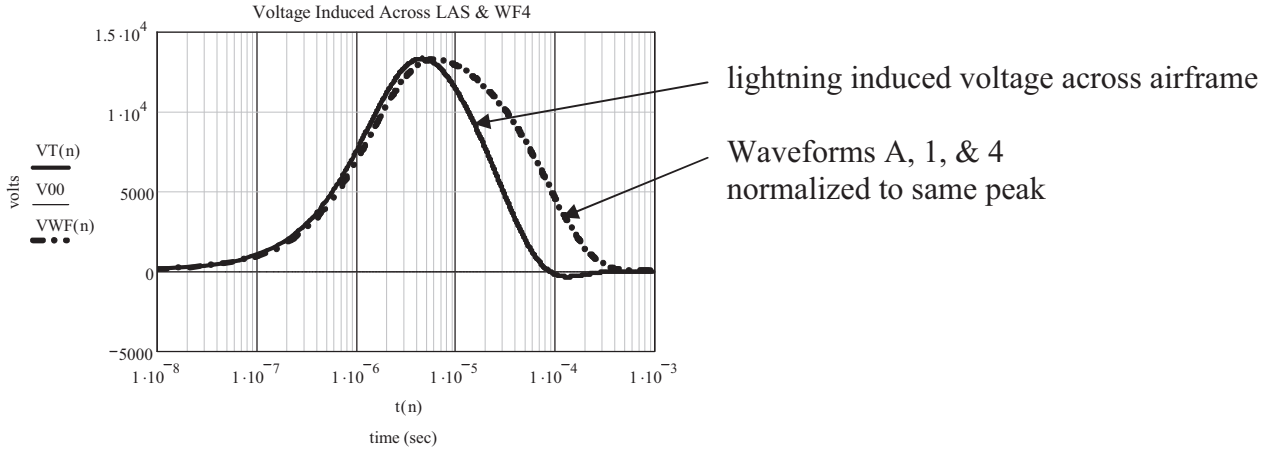

Figure 3 Induced Voltage across the Composite Airframe with a Braid Cable

Note that the 13kV peak is less than the 20kV peak that would result from the 200kA through the 100mΩ composite airframe alone. Aircraft designers install a low inductance groundplane to reduce the voltage more as will be shown, below, in Figure 14.

The current through the CFC and the braid in the frequency domain are as follows:

$$\widetilde{I}_{CFC}(s) = \frac{\widetilde{V}(s)}{\widetilde{Z}_{CFC}(s)} = I_0 \cdot \frac{L_{braid}}{L_{CFC}+L_{braid}} \cdot \left(\frac{1}{s+a} - \frac{1}{s+b}\right) \cdot \frac{s+\alpha}{s+\gamma} \tag{5}$$

and

$$\widetilde{I}_{braid}(s) = \frac{\widetilde{V}(s)}{\widetilde{Z}_{CFC}(s)} = I_0 \cdot \frac{L_{CFC}}{L_{CFC}+L_{braid}} \cdot \left(\frac{1}{s+a} - \frac{1}{s+b}\right) \cdot \frac{s+\beta}{s+\gamma} \tag{6}$$

Note that the system parameter in the denominator is the loop time constant, γ^{-1}.

The inverse Laplace transforms of these currents are as follows:[3]

Currents in the composite skin are $I_{skin} = I_{as} - I_{bs}$, where

$$I_{as}(t) = I_0 \cdot \frac{L_{braid}}{L_{skin} + L_{braid}} \cdot \left\{ \frac{\left[a^2 - a \cdot (\alpha + \beta) + \alpha \cdot \beta\right] \cdot e^{-a \cdot t}}{(\alpha - a) \cdot (\gamma - a)} + \frac{\left[\gamma^2 - \gamma \cdot (\alpha + \beta) + \alpha \cdot \beta\right] \cdot e^{-\gamma \cdot t}}{(\alpha - \gamma) \cdot (a - \gamma)} \right\} \tag{7}$$

$$I_{bs}(t) = I_0 \cdot \frac{L_{braid}}{L_{skin} + L_{braid}} \cdot \left\{ \frac{\left[b^2 - b \cdot (\alpha + \beta) + \alpha \cdot \beta\right] \cdot e^{-b \cdot t}}{(\alpha - b) \cdot (\gamma - b)} + \frac{\left[\gamma^2 - \gamma \cdot (\alpha + \beta) + \alpha \cdot \beta\right] \cdot e^{-\gamma \cdot t}}{(\alpha - \gamma) \cdot (b - \gamma)} \right\} \tag{8}$$

Currents in the internal braid are $I_{braid} = I_{ab} - I_{bb}$, where

$$I_{ab}(t) = I_0 \cdot \frac{L_{skin}}{L_{skin} + L_{braid}} \cdot \left\{ \frac{\left[a^2 - a \cdot (\alpha + \beta) + \alpha \cdot \beta\right] \cdot e^{-a \cdot t}}{(\beta - a) \cdot (\gamma - a)} + \frac{\left[\gamma^2 - \gamma \cdot (\alpha + \beta) + \alpha \cdot \beta\right] \cdot e^{-\gamma \cdot t}}{(\beta - \gamma) \cdot (a - \gamma)} \right\} \tag{9}$$

$$I_{bb}(t) = I_0 \cdot \frac{L_{skin}}{L_{skin} + L_{braid}} \cdot \left\{ \frac{\left[b^2 - b \cdot (\alpha + \beta) + \alpha \cdot \beta\right] \cdot e^{-b \cdot t}}{(\beta - b) \cdot (\gamma - b)} + \frac{\left[\gamma^2 - \gamma \cdot (\alpha + \beta) + \alpha \cdot \beta\right] \cdot e^{-\gamma \cdot t}}{(\beta - \gamma) \cdot (b - \gamma)} \right\} \tag{10}$$

These two currents on the skin and braid add up to the lightning current.

For a simple circuit with two parallel paths of resistance and inductance, driven by a double exponential current, the final results are complicated. The loop inverse time constant, $\gamma = (R1+R2)/(L1+L2)$, plays a ubiquitous role in all of these results including pulling some waveforms below zero at late times.

The resulting lightning current division between the composite skin and the braid are shown in Figure 4.

Note that the early time, higher frequency, current travels through the composite skin and the late time, lower frequency, travels through the interior braid. That late time braid current is defined as Waveform 5 (WF5) in the SAE and RTCA/DO-160 documents[4, 5], that is, rising in 40-50μs and decaying in 100-500μs. That low frequency nature of the induced current on the braid is what allows it to diffuse through normal copper braid shields with less than 20AWG wires, rendering the braid another parallel impedance in the total circuit with negligible shielding effectiveness.

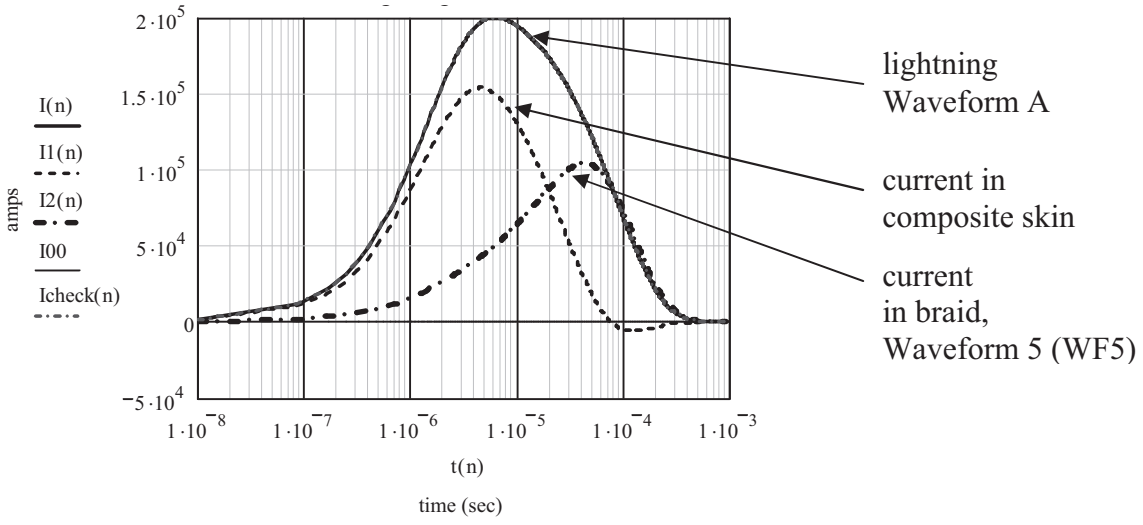

Figure 4 Lightning Current Division between Composite Skin and a Braid Cable Shield

Note in this example that the peak braid current is 100kA.

Misunderstanding about this phenomenon exists because of what the current source imposes on the distribution of currents and their waveforms as opposed to a voltage source.

Take the same two parallel RL branches driven by a notional voltage source and a notional current source and see what the braid current looks like:

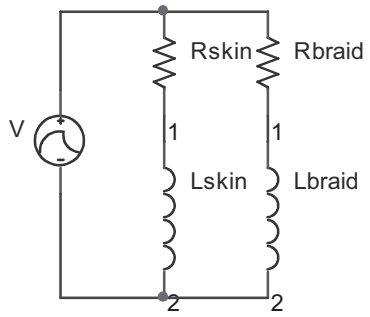

Figure 5 Notional Voltage Source Driving the Parallel RL Branches

The current through the braid branch is the following, dominated by the braid RL time constant, β^{-1}:

$$\widetilde{I}_{braid}(s) = \widetilde{V}(s) \cdot \frac{1}{L_{braid} \cdot (s + \beta)} \tag{11}$$

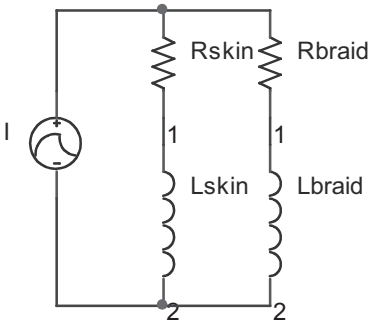

Figure 6 Notional Current Source Driving the Parallel RL Branches

The current through the braid branch is the following, dominated by the loop RL time constant, γ^{-1}:

$$\widetilde{I}_{braid}(s) = \widetilde{I}(s) \cdot \frac{L_{skin}}{L_{skin} + L_{braid}} \cdot \frac{s + \alpha}{s + \gamma} \tag{12}$$

It is the parallel paths of the two branches driven by a common current source that results in the low frequency Waveform 5 on the shield dominated by the loop time constant. The voltage source with the same waveform as the lightning source would induce a current on the braid that whose rise time would be dominated by the braid time constant. Therein lies the difference between conventional intuition and this unique lightning phenomenon.

COAXIAL CABLE SHIELDING

In 1934, Schelkunoff analyzed the shielding characteristics of coaxial cable shields.[1] Therein, solving the boundary value problem for cylindrical conductors serving as coax shields, shown in Figure 7, Schelkunoff wrote the coupled equations, 13 & 14, below, for the electric fields induced along the interior and exterior surfaces due to currents in the exterior and interior surfaces.

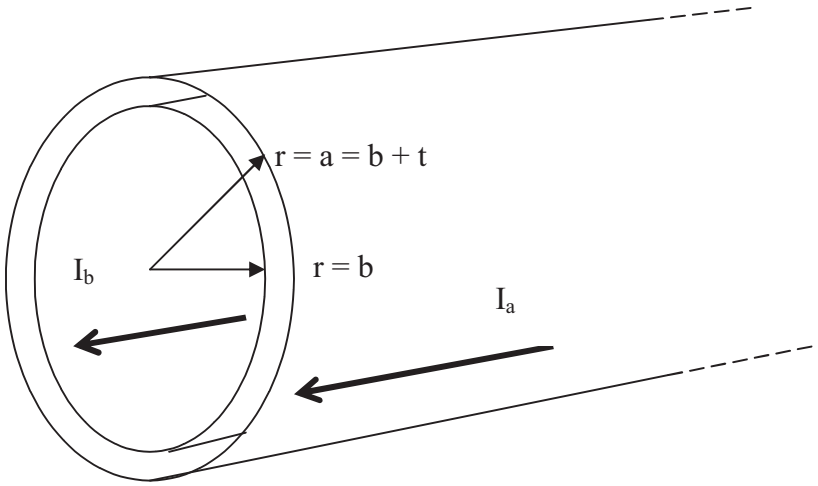

Figure 7 Cylindrical Coaxial Shield

Schelkunoff's coupled shield impedance equations, $E_a = I_a \cdot Z_a + I_b \cdot Z_{ba}$ (13)

$$E_b = I_a \cdot Z_{ab} + I_b \cdot Z_b \quad (14)$$

where
I_a is the current on the outer surface, r = a;
I_b is the current on the inner surface, r = b;
Z_a is the surface impedance of the exterior surface of radius a;
Z_b is the surface impedance of the interior surface of radius b; and,
$Z_{ab} = Z_{ba}$ is the transfer impedance, Z_T, between the two surfaces, that is the electric field induced on one surface due to a current on the other.

From eqns. 13 & 14, when there is no internal source current, $I_b = 0$, and the frequency is so low that the surface impedance equals the transfer impedance, $Z_a = Z_{ab}$, the induced electric field along the inner surface is the same as the induced electric field on the outer surface, $E_a = E_b$, the first contention of this essay with the same conclusion regarding the induced end-to-end voltages, $V = \int_0^l E \cdot dz$.

From Schelkunoff[1], with some notation changes reflecting modern usage[2], these impedances are as follows including high frequency approximations (good to very low frequencies)[1, 2]:

inner surface impedance: $\widetilde{Z}_b = \frac{\eta}{2 \cdot \pi \cdot b} \cdot \frac{\left[J_0(k \cdot b) \cdot N_1(k \cdot a) + J_1(k \cdot a) \cdot N_0(k \cdot b)\right]}{D}$ (15)

high frequency approximation: $\widetilde{Z}_b \cong \frac{1}{2 \cdot \pi \cdot b \cdot t \cdot \sigma} \cdot \frac{\sqrt{i\omega \cdot \tau_d}}{\tanh\left(\sqrt{i\omega \cdot \tau_d}\right)} \cong \frac{1}{2 \cdot \pi \cdot b \cdot t \cdot \sigma} + \frac{1+i}{2 \cdot \pi \cdot b \cdot \delta \cdot \sigma}$ (16)

outer surface impedance: $\widetilde{Z}_a = \frac{\eta}{2\cdot\pi\cdot a}\cdot\frac{\left[J_0(k\cdot a)\cdot N_1(k\cdot b)+J_1(k\cdot b)\cdot N_0(k\cdot a)\right]}{D}$ (17)

high frequency approximation: $\widetilde{Z}_A \cong \frac{1}{2\cdot\pi\cdot a\cdot t\cdot\sigma}\cdot\frac{\sqrt{i\omega\cdot\tau_d}}{\tanh\left(\sqrt{i\omega\cdot\tau_d}\right)} \cong \frac{1}{2\cdot\pi\cdot a\cdot t\cdot\sigma}+\frac{1+i}{2\cdot\pi\cdot a\cdot\delta\cdot\sigma}$ (18)

transfer impedance: $\widetilde{Z}_{ab} = \frac{k}{2\pi\cdot a\cdot\sigma}\cdot\frac{J_1(k\cdot b)\cdot N_0(k\cdot b)+J_0(k\cdot b)\cdot N_1(k\cdot b)}{D} = \frac{1}{2\cdot\pi\cdot\sigma\cdot b\cdot a\cdot D}$ (19)

high frequency approximation: $\widetilde{Z}_{ab} \cong \frac{1}{2\cdot\pi\cdot\sqrt{a\cdot b}\cdot t\cdot\sigma}\cdot\frac{\sqrt{i\omega\cdot\tau_d}}{\sinh\left(\sqrt{i\omega\cdot\tau_d}\right)} \cong \frac{e^{-(1+i)2\cdot t/\delta}}{2\cdot\pi\cdot\sqrt{a\cdot b}\cdot t\cdot\sigma}$ (20)

where

J_n and N_n are Bessel functions of first and second kind, order n, respectively,
$a = b + t$, where the braid thickness, t << b < a,
$k = \sqrt{i\omega\cdot\mu\cdot\sigma} = (1+i)\cdot/\delta$, the wave number in the conductor,
δ is the skin depth, $\delta = \sqrt{1/\pi\cdot\mu\cdot\sigma\cdot f}$, and $\omega\cdot\tau_d = 2\cdot t^2/\delta^2$,
τ_d is the diffusion time constant through the cylinder/shield wall, $\tau_d = \mu\cdot\sigma\cdot t^2$,
$\eta = \sqrt{i\omega\cdot\mu/\sigma}$ is the wave impedance in the conductor ($\sigma >> \omega\cdot\varepsilon$),
$Z_{ab} = Z_{ba} = Z_T$, and the denominator, above, is

$$D = J_1(k\cdot b)\cdot N_1(k\cdot a) - J_1(k\cdot a)\cdot N_1(k\cdot b) \quad (21)$$

The two surface impedances approximate to the DC resistance plus a √f skin depth effect. The transfer impedance approximates to the DC resistance times an exponential decay through the coax wall according to the √f skin depth effect, also. When the skin depth exceeds the coax shield thickness, the surface impedances and the transfer impedances become the same, the resistance of the coax shield. The two are plotted below in Figure 8 for a copper 40AWG wire braid shield, showing that the transfer impedance diverges from the surface impedances when $\omega \geq \tau_d$. For a Waveform 5 induced lightning current on the braid with a rise time of 40-50μs and a fall time of 88μs, the induced voltage in the shield is therefore the same inside and out. Furthermore, the IR-drop voltage across the composite skin controls that across the braid. In order to obtain any shielding effectiveness from a braid shield to such an environment, the wire braid would have to be larger than 20AWG, impractical for widespread use in aerospace vehicles. The solution is the addition of a high-mu foil to be discussed below.

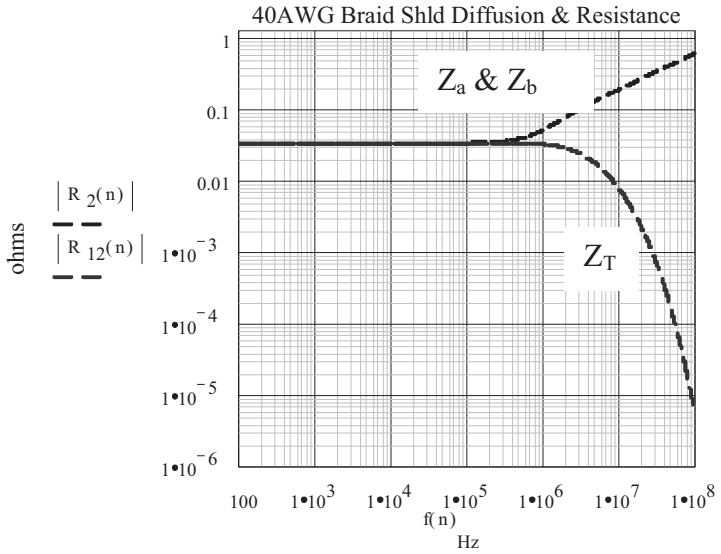

Figure 8
Surface Impedances and Transfer Impedance for a 40AWG Wire Braid Coaxial Shield

SIMPLE CIRCUIT MODEL OF LOW FREQUENCY CURRENT DIVISION AND CABLE SHIELDING

A new low frequency simple circuit model of the combined composite skin and the braid shielded circuit that includes the above diffusion effects is shown in Figure 9, below, for $\omega \cdot \tau_d \geq 1$. This is not the usual higher frequency transfer impedance. When $\omega \cdot \tau_d < 1$, the internal, external, and shield transfer impedances merge into one parallel impedance, $Z_a = Z_b = Z_T$, connected to structure at both ends, shown in Figures 2 & 10. Note that $\omega \cdot \tau_d = 2 \cdot t^2/\delta^2$.

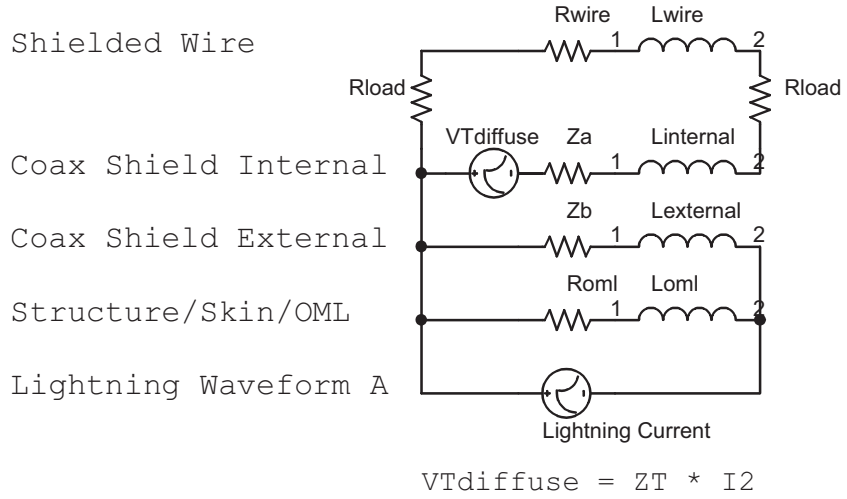

Figure 9 Simple Low Frequency IR-Drop Circuit Model for Coax Shielding when $\omega \cdot \tau_d \geq 1$

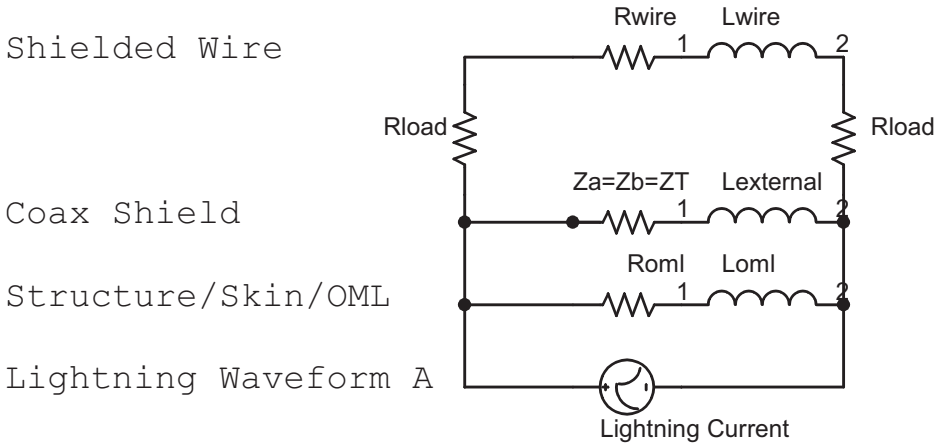

Figure 10 Simple Low Frequency IR-Drop Circuit Model for Coax Shielding when $\omega \cdot \tau_d < 1$
The Most Common Situation in Composite Airframes with WF5 on the Copper Braid(s)

Justification for the model in Figures 2 and 10 is that the current distribution through the braid becomes uniform when $\omega \cdot \tau_d \leq 1$ thereby making the induced longitudinal electric field, E_z, and the induced voltage, V, the same, inside and out. The current distribution is shown in Figure 11, below, for $\omega \cdot \tau_d = 10^2$, 10, 1, 10^{-1}, and 10^{-2}. This shows that the current is almost uniform through the braid by the time $\omega \cdot \tau_d = 1$.

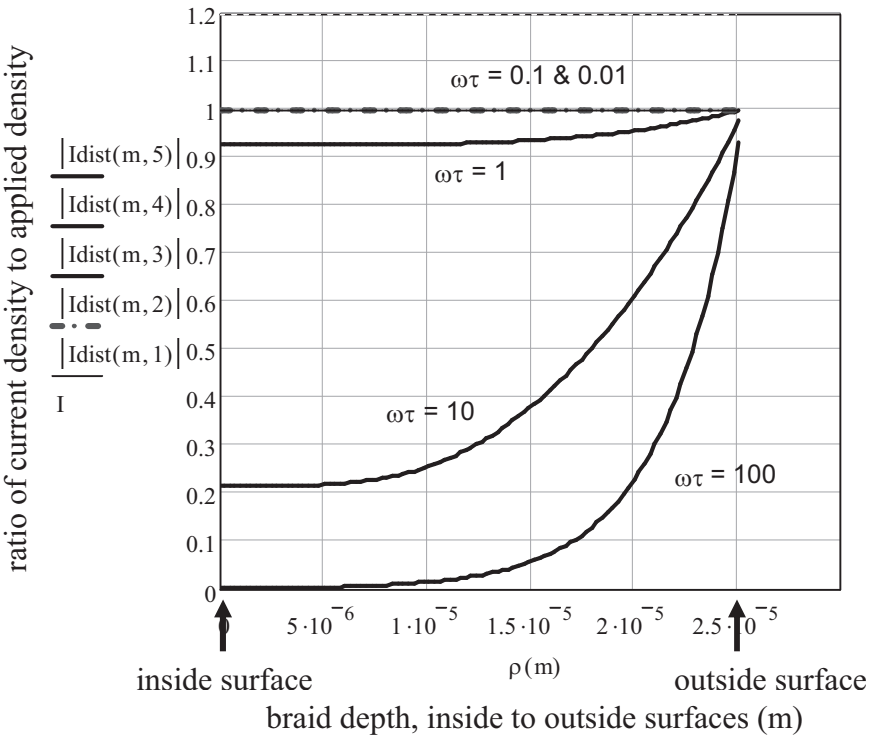

Figure 11 Current Distribution through Copper Braid/Foil for Different Frequencies Relative to the Diffusion Time, τ, when a Current is Impressed on the Outer Surface

Let's look at three different system configurations to see how much voltage is induced end-to-end with different system design relative to the two parallel RL branches.

The three exponential terms contributing to the voltage in the above composite airframe and single braid look as follows in Figure 12 which include the lightning rise term, $e^{-a \cdot t}$, the lightning decay term, $e^{-b \cdot t}$, and the circuit loop term, $e^{-\gamma \cdot t}$, $\gamma = \dfrac{R1 + R2}{L1 + L2}$.

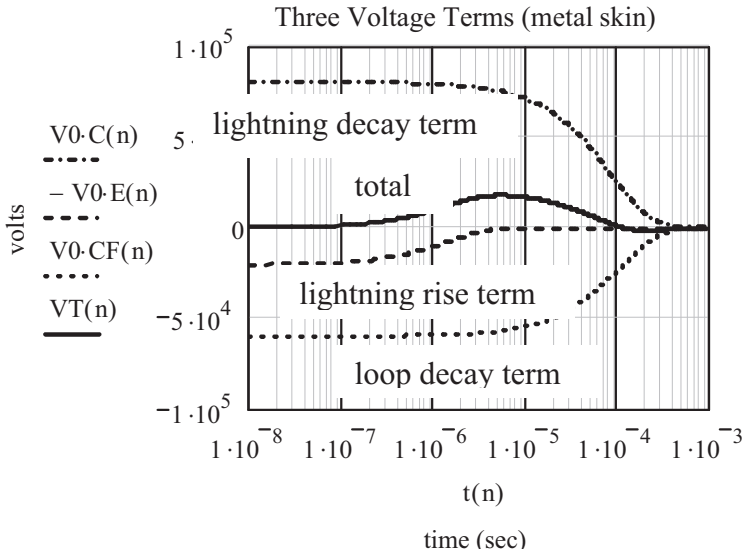

Figure 12 The Three Terms comprising the above Induced Voltage in the Composite Skin

Note how the loop term reduces the peak voltage for this set of parameters and causes it to swing negative at late times.

If the skin resistance is reduced by two orders of magnitude to, say, that of titanium, the induced voltage with its three exponential terms are as follows in Figure 13:

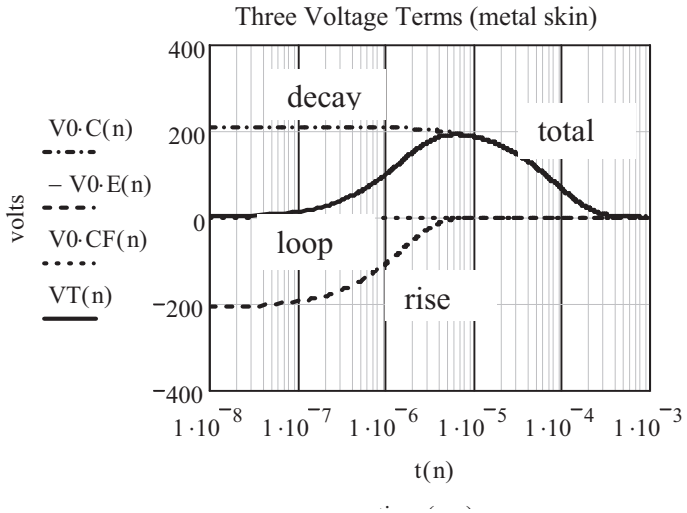

Figure 13 Induced Voltage with Titanium Skin

Note that the loop term has all but disappeared because the skin is conducting most of the current.
Note that the peak voltage has dropped from about 13kV to 180V or 41dB. If the skin were aluminum, the induced voltage would drop another 20dB. Titanium has some advantage over aluminum against direct strike damage because of its thermal properties particularly when covered with paint and thermal protection materials as in some space vehicles.

If the airframe remains composite, that 41-61dB of protection must be made up somewhere else. That make up in protection will add weight, a difficult point to make when management is overly weight conscious and so proud of the weight savings derived from the use of composites.

If the braid inductance is reduced to, say, 600nH like groundplane in aircraft fuselages are designed, the induced voltage and its three exponential terms look as follows in Figure 14:

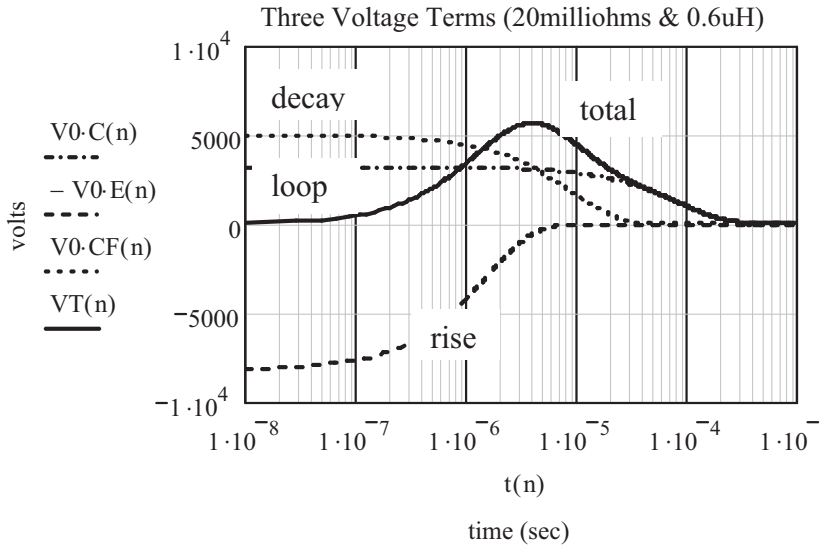

Figure 14 Induced Voltage with Low Inductance Groundplane

Note that the peak voltage has dropped from 13kV down to about 5.6kV or 11dB and, as important, the voltage is now controlled by the braid/groundplane with its linear properties instead of the nonlinear composite structure and its nonlinear joint impedances arcing and tracking with increased lightning amplitudes. This makes verification with the low level system level test easier and the extrapolation more credible. Power line surge protection must still be rated at 10kA or higher.

SUMMARY OF SIMPLE MODELING

The models in Figures 2 & 10 provide accurate numbers for the induced open circuit voltage and short circuit current in a shielded wire or an unshielded wire, e.g. the induced voltage will be that developed across the parallel circuit of conductors and the composite airframe, dominated by the composite airframe. The braid shield acts as another impedance across the structure, lowering the induced voltage at the shielded wire loads only a small amount.

This method of modeling and analysis in this paper is recommended as a supplement to and/or correction of SAE ARP5415A, Appendix B.1.1, and the associated text and circuit models with regard to the composite IR-drop induced voltages and currents in shielded and unshielded wires in composite airframes. The individual parameters must be determined for each system. This modeling technique has been criticized because of its simplicity, however it agrees with test data. This paper is intended to provide a theoretical basis for the simple model in the frequency range we are dealing with.

A new cable shield design is presented, below, for shielding the low frequency WF5 induced lightning currents on cable shields, the actual configuration and shield grounding a first in this field.

A solution for this problem is high-mu foil under the copper braid that has a skin depth small enough to actually shield the low frequency Waveform 5 currents. The high-mu foil must be overlapped by, say, 20-30% to maintain contact, maximize optical coverage, and keep the magnetic reluctance down.

The possible drawback is saturation from high currents of the high-mu material rendering it ineffective, also. A comparison of the shielding by a foil the same thickness as the copper foil braid is shown below in Figure 15. The nickel doesn't have high enough permeability to improve the attenuation down to Waveform 5 frequencies. The mu-metal with $\mu_r \geq 10{,}000$ lowers the diffusion curve below the 10-25 kHz frequencies in order to attenuate Waveform 5. The high frequency transfer inductance is not shown in order to highlight the low frequency diffusion. Besides, the foil lowers the transfer inductance by 20dB or more as seen in the Raychem data in Figure 16. The high-mu metals are ferrous-nickel alloys therefore their conductivity is at least 3-5 times lower than copper.

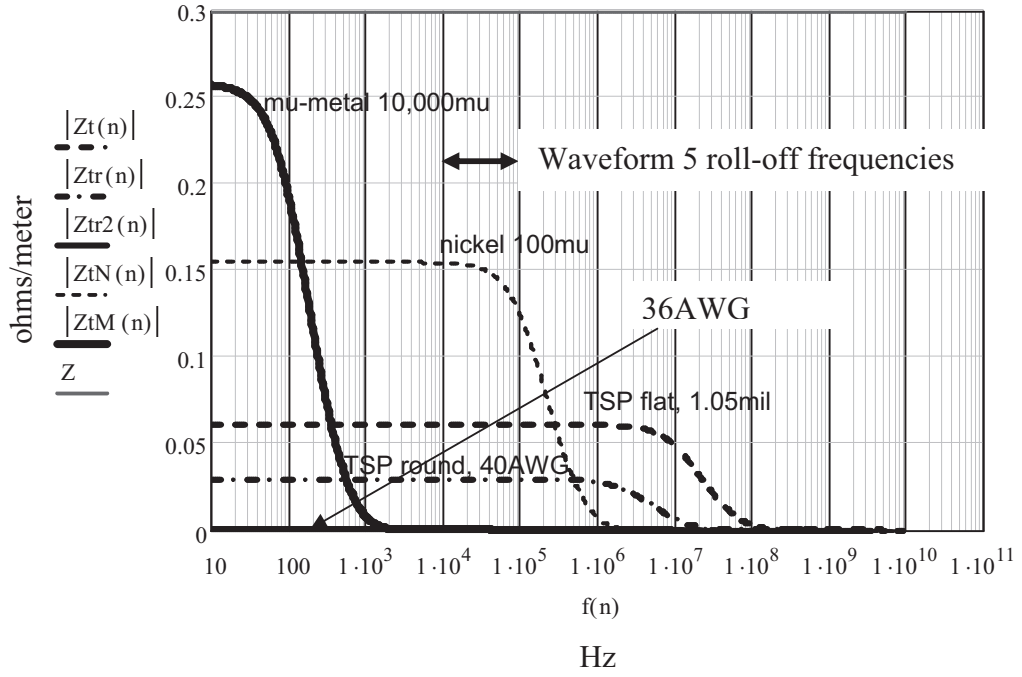

Figure 15 Copper Braid versus High-Mu Foil for Low Frequency Shielding

The high-mu foil roll-off frequency must be below the lightning Waveform 5 roll-off frequencies in order to attenuate the Waveform 5 current. This is illustrated in the time domain attenuation shown below in Figure 16 for the above transfer impedance diffusion curves.

This example with a 1 mil hi-mu foil, the improvement over a copper 1 mil foil braid is 17dB at 10kHz and 70dB at 25kHz, the roll off frequencies for a Waveform 5 current.

Raychem makes a "superscreen" with one and two high-mu foil layers and have published the following data, Figure 20, showing the dramatic improvement in low frequency shielding[9]. With another layer of braid and foil, Raychem shows another 60dB improved shielding, 10-25kHz.

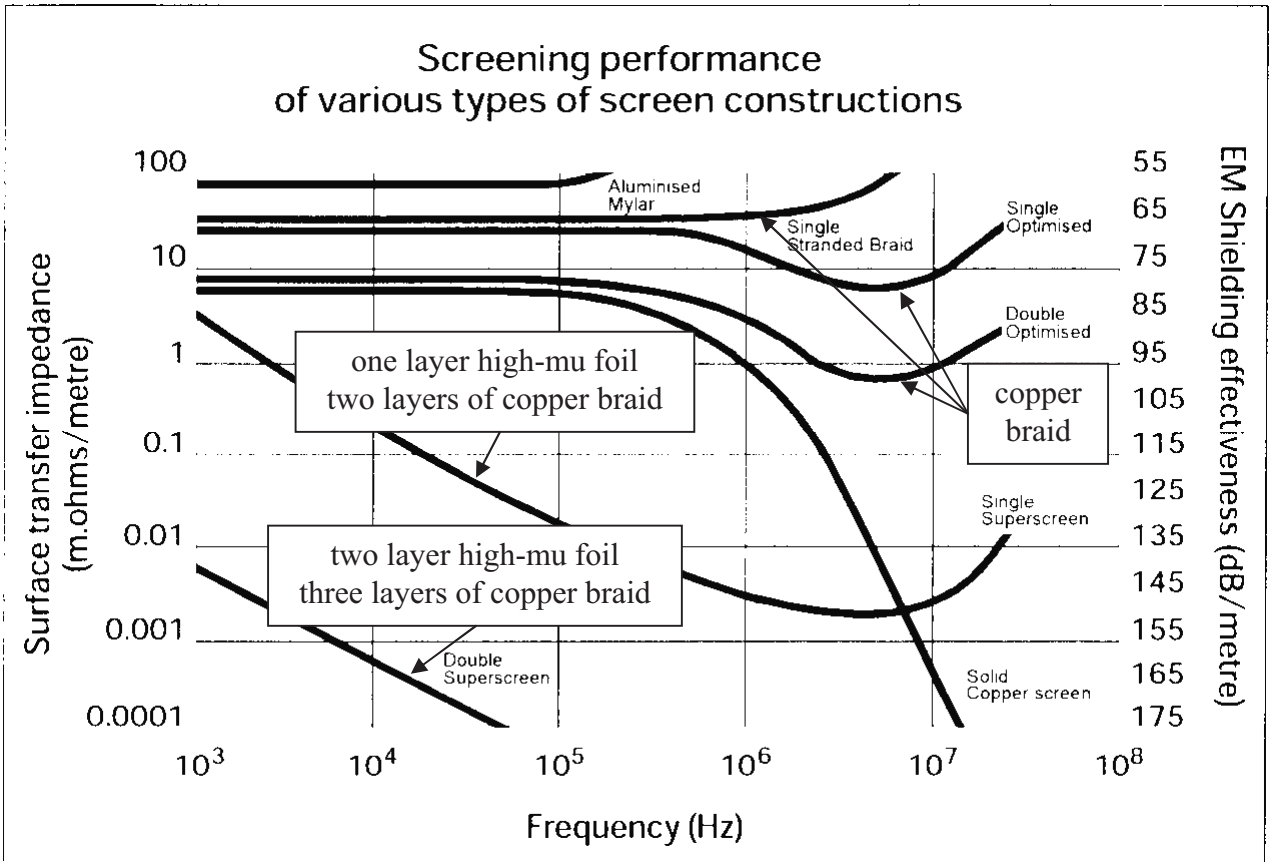

Figure 16 Raychem "Superscreen" with High-Mu Foil Compared to Copper Braid[8]
(See Figure 18 for superscreen cables with high-mu foil.)

D. E. Merewether modeled the saturation effects of ferromagnetic materials used in coax shields[6, 7]. A notional graph of such effects is in Figure 17, B versus μ(H)·H, showing the sharp drop in relative permeability above the saturation field level, B_S. That renders the foil much less of a shield above some level of induced current/field. A real graph with data is in Figure 18 where B_S is fuzzier.

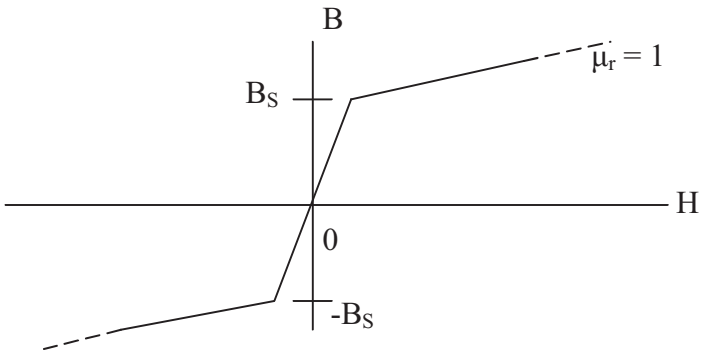

Figure 17 Notional Graph of Ferromagnetic Saturation Effect

As the field increases and the mu-metal saturates, its permeability eventually decreases to that of free space, i.e. $\mu_r \rightarrow 1$.[2]

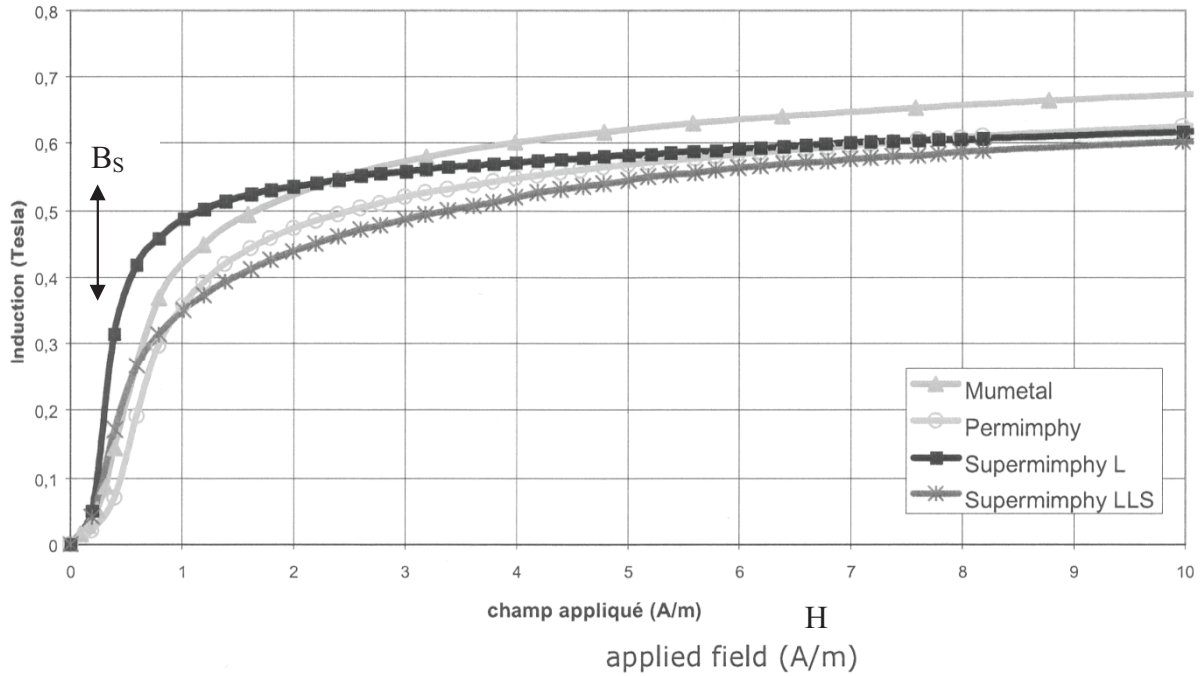

DC magnetization curves for Mumetal, Permimphy, Supermimphy L and Supermimphy LLS.

Figure 18 Typical High-Mu Metal Magnetization Curves from ArcelorMittal[9]

Merewether developed a simple prescription to see how thick of a foil was needed before it was saturated all the way through using a damped sinusoid.

$$t_S \approx \frac{1}{\pi} \cdot \sqrt{\frac{I_p}{\sigma \cdot B_S \cdot f \cdot R}} \tag{22}$$

where

I_p is the peak current,
σ is the conductivity,
B_S is the material's saturation level,
f is the frequency,
t_s is the foil thickness to prevent total saturation, and
R is the cable shield radius.

Lightning Waveform 5 is not sinusoidal. However, we will use this simple prescription until we derive a better one. Its rise time is 40μs corresponding to a frequency of about 25kHz. Its fall time is about 88μs corresponding to a frequency of 10kHz. Its conductivity is about x5 less than copper or roughly 10^7 mhos/m. The saturation level used here is 1.53W/m^2, the same as Merewether used. With a peak current of 1kA at 25kHz, all of this gives us a minimum foil thickness of 1mm or 2.54 mils, close to the thickness of a 40AWG wire. More investigation will come up with the best material with the least weight penalty including a copper overbraid to absorb most of the current and perhaps another layer of foil as in the Raychem example. This example is too crude to use for design, meant only to "ballpark" the numbers from Merewether's model, the 2½ mils being a good sign. A copper overbraid the same thickness would reduce the current in the high-mu foil by about 600, therefore about 1 mil thickness would suffice for this example. The above Raychem foil is 2 mils thick[11]. The attenuation at high frequencies in the high-mu foil is close to 1/200 or 46dB.

As an example, the induced lightning voltage from a Waveform 5 current in a 1 mil foil shield is shown below in Figure 19 for a range of relative magnetic permeability, μ_r, from about 1-to-10,000. When the transfer impedance diffusion curve starts rolling off below 10kHz, we see some real attenuation of the WF5 pulse. The voltages were relatively unchanged with μ_r = 1-10 because the transfer impedance was still outside the lightning spectrum even with a factor of x10 difference in permeability. Relative permeability as much as 10,000 or more are routine therefore the attenuation can be increased to whatever level is needed as long as saturation is prevented. From the much longer rise time of the high-mu attenuated voltage, we clearly have a new waveform to define, say Waveform 5C, with a rise time of about 120μs and a longer fall time. That may drive up our capital test equipment expenses or we just shape the output of present pulsers.

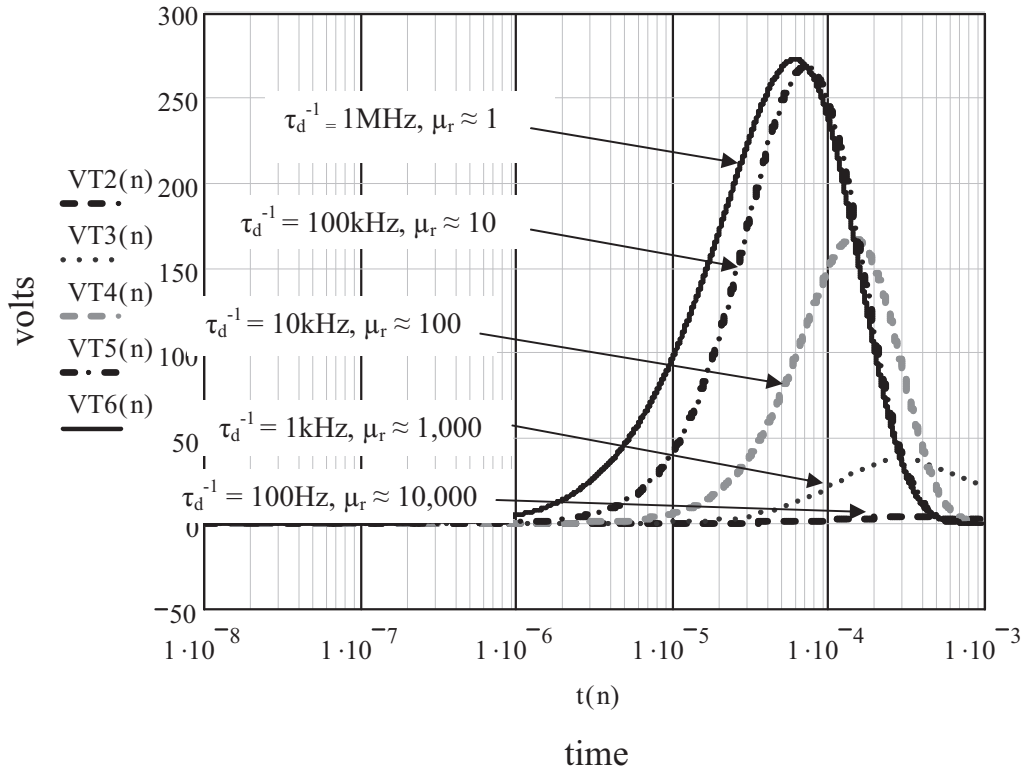

Figure 19 Relative Attenuation of a WF5 Current with Varying Permeability 1 mil Cable Shield

These results are high because we used a simple f^{-1} roll off, eqns. 24, below, instead of the difficult exponential roll off therefore not attenuating the higher frequencies enough.

$$V(t) = \int ds \cdot e^{s \cdot t} \cdot \widetilde{Z}_T(s) \cdot \widetilde{I}_{shld}(s) \tag{23}$$

where I_{shld} is a 1kA Waveform 5 current and

$$Z_T \approx R_{DC}/(1 + s \cdot \tau_d) \tag{24}$$

We need to add a layer of copper braid on top of this in order to reduce the current on the high-mu foil by about 600 and the induced voltage by the same. This may be a bigger reduction when skin depth is

considered; see Figure 19. The layered shield problem is not trivial[1] although we can ballpark it simplistically.

The trade off then includes the following parameters: (1) one or more layers of copper braid and/or foil, (2) foil permeability, (3) foil saturation level, (5) foil conductivity, and (6) foil thickness. The Raychem superscreen cable was allegedly developed for lightning protection on a very big Boeing airplane.[11]

The superscreen cable has a possible flaw; that is, the inner copper braid (fig. 20) could conduct current around the high-mu foil, thereby negating the shielding by the foil. Test results then show low frequency shielding more like a 30AWG copper braid than a high-mu foil.[10] Installing any copper shield underneath the high-mu foil will do the same thing. The solution is to isolate the inner braid from the high-mu foil and ground the inner copper braid at one end only as Raychem has done per the information in this paper.[21] Make the inner shield a low weight thin copper foil so the wiring has a low loss shield around it. Eliminate the middle Cu braid on the double superscreen.

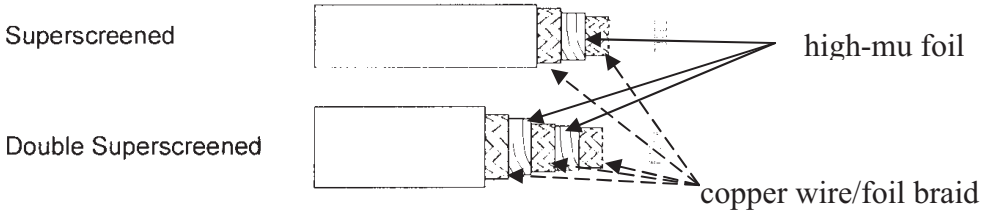

Figure 20 Raychem Superscreen Shielded Cables[9]

We need the copper braid or foil next to the wires because the high-mu foil is too lossy due to (1) the DC resistance and (2) the reduced skin depth. The two surface impedances are shown in Figure 21 where the impedance of the high-mu foil is about x600 (58dB) higher than the copper braid.

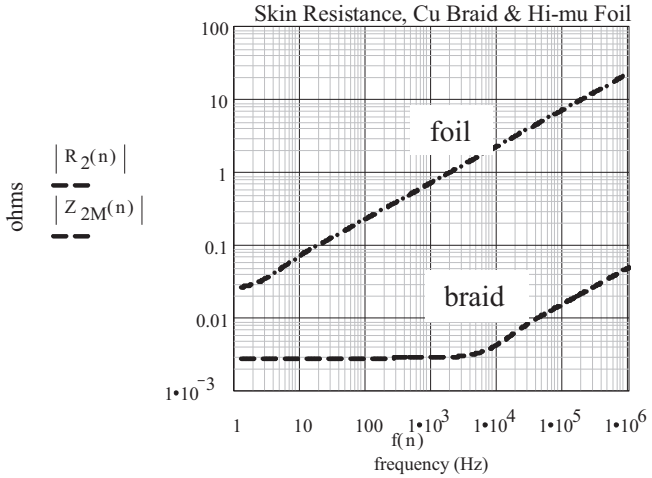

Figure 21 Impedance of Copper Braid and High-mu Foil

This large difference in resistance will enhance the apparent shielding effectiveness more than with either the copper or foil by themselves, i.e. it will be this ratio times the transfer inductance of the foil.

DETAILS OF LAYERED COPPER BRAID & HIGH-MU FOIL WITH INNER COPPER LAYER

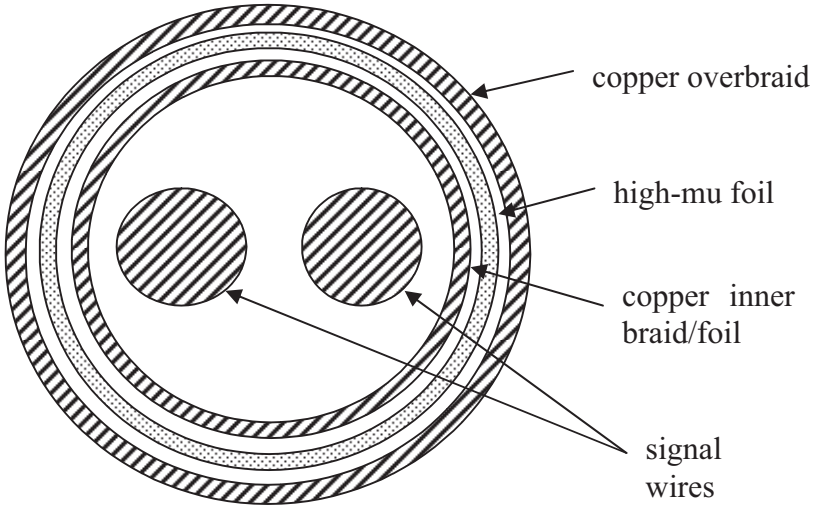

Figure 22 WF5 Cable Design: Copper Overbraid, High-mu Foil, & Copper Inner Braid/Foil Insulation on & in between all Surfaces[21]

Figure 23 Grounding Scheme for the WF5 Cable Shield Design Inner Layer grounded at One End Only[21]

Figure 24 is the system circuit model including the layered copper braid and high-mu foil. Figure 25 is a simplified circuit driving the layered shield with a Waveform 5 current. The innermost braid has been left out since we will ground it at one end only, effectively removing it from this shield diffusion model.

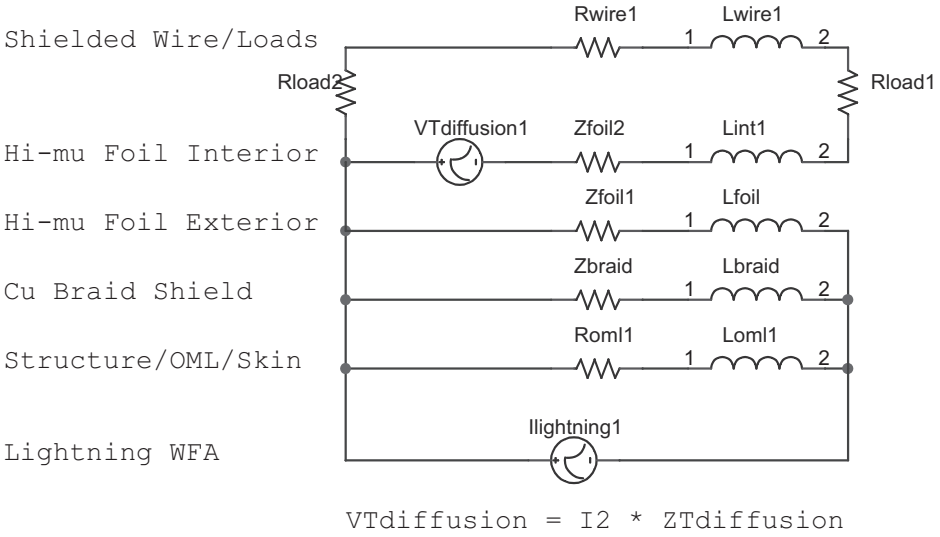

Figure 24 System Circuit Model with Cu Braid & High-mu Foil Wire Shield

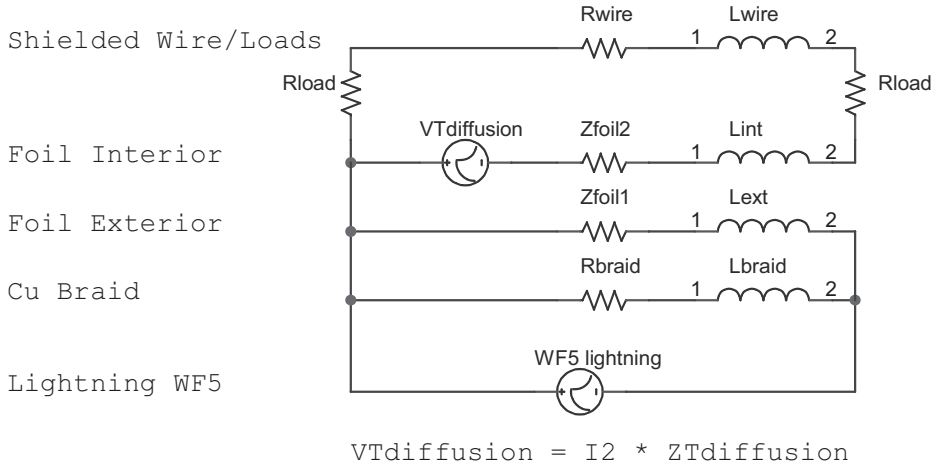

Figure 25 Simplified Circuit Model Driving Shield with WF5 Current
Assumes $\omega \cdot \tau_d \leq 1$ in the Copper Braid, $\omega \cdot \tau_d \geq 1$ in the Foil
Used to Evaluate Cu Braid & Foil Parameters

The induced voltage, $V_{Tdiffusion}$, is the following in the frequency domain, illustrating the enhancement due to the impedance difference between the copper braid and the high-mu foil in Figure 26:

$$V_T = \frac{Z_{braid}}{Z_{braid} + Z_{foil}} \cdot Z_{Tfoil} \cdot I_{WF5} \tag{25}$$

where over the frequency range of interest, 10-10^5 Hz, the ratio of impedances which is the ratio of currents is about $\sqrt{\frac{\sigma_{braid}}{\mu_{r(foil)} \cdot \sigma_{foil}}} \approx \frac{1}{600}$ and the foil transfer impedance is about $R_{foil} \cdot e^{-2 \cdot t/\delta} \approx 2.5 m\Omega / m$ resulting in an equivalent transfer impedance of 40μΩ/m or about 128dB shielding attenuation, consistent with Raychem's advertised results in Figure 14. The actual ratio of currents is shown in Figure 26, the foil transfer impedance in Figure 27. Waveform 5 current is shown in Figure 3.

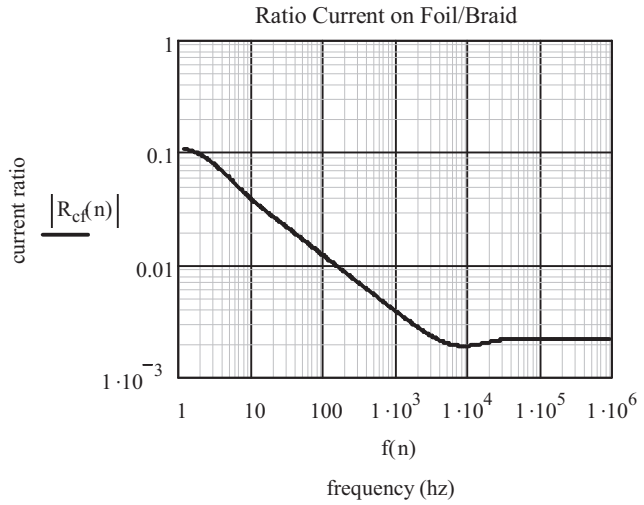

Figure 26 Ratio of Current on High-mu Foil/Copper Overbraid

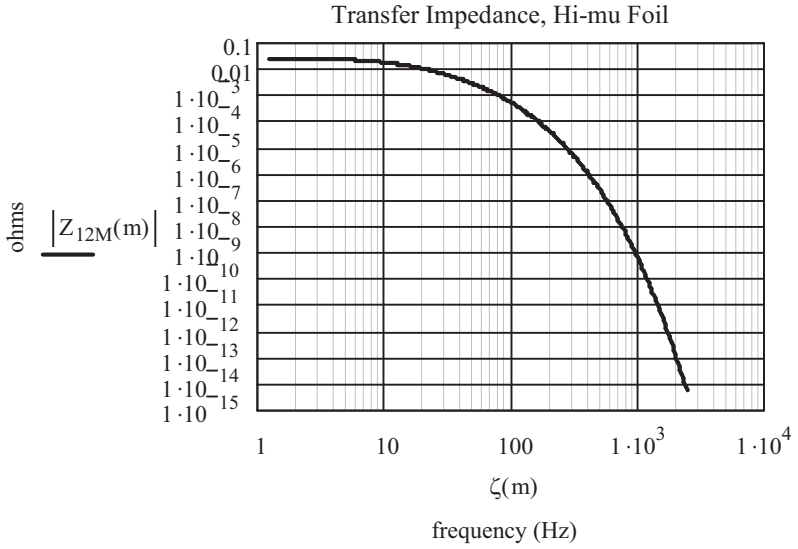

Figure 27 Transfer Impedance of High-mu Foil

The equivalent transfer impedance of the two layers of shielding is the product of the above two functions. The voltage induced when a current is applied to the layered shield is as follows:

$$V_T(t) = \int_0^{\infty} ds \cdot e^{s \cdot t} \cdot \frac{\widetilde{Z}_{braid}(s)}{\widetilde{Z}_{braid}(s) + \widetilde{Z}_{foil}(s)} \cdot \widetilde{Z}_{Tfoil}(s) \cdot \widetilde{I}_{WF5}(s) \tag{26}$$

The shielding effectiveness of the high-mu foil is considerably enhanced and saturation of the foil is greatly decreased by the copper overbraid due to the resulting reduction of current on the foil.

A quick and dirty approximation to the above induced voltage in Equation 26 was obtained by simply multiplying the answers in Equation 23 and Figure 19 by a constant ratio of 400 interpreted to be the ratio of currents on the copper braid over the current on the high-mu foil instead of the frequency dependent response in Figure 26, shown in Figure 28, below. The log-log graph was used to better show the difference in the peak voltages. This needs to be performed more precisely with better tools.

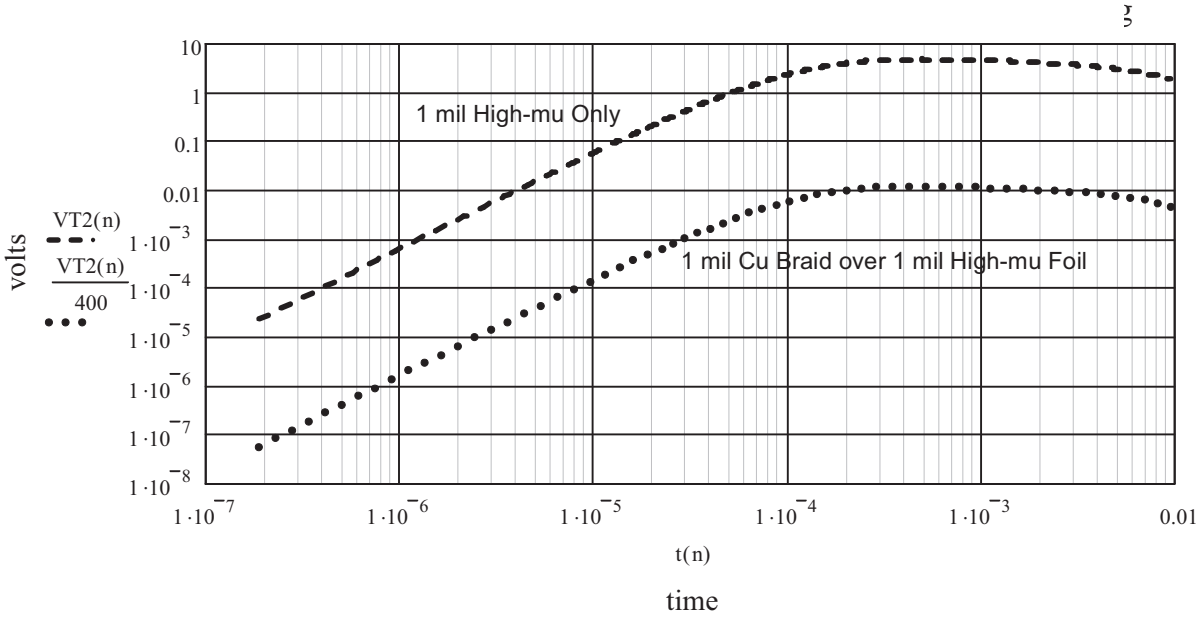

Figure 28 Comparison of Shielding from a High-mu Foil to a Cu Braid over the Foil

The transfer impedance of the cable shield alone from peak induced voltage to peak Waveform 5 current is therefore 10 micro-ohms per meter. That will attenuate the 100kA Waveform 5 current in Figure 4 to 1V/m.

The combined cable shield is so good that the overall shielding effectiveness will be controlled by the joints at the connectors. A layered boot with high-mu film would be necessary to come close to the cable shield itself. These numbers will increase when 5-10mΩ connectors are included, in fact increase to about 5-10V for a 1kA shield current.

EFFECTS OF THE OPEN SHIELD ON THE DIFFERENTIAL & COMMON MODE SIGNALS

There is a serious question about the effects of the inner copper layer being open at one end on the signals passing through. We will hand-wave it for now and refine it and test later. It will have to be addressed in the signal error budget of the circuit designers similar to the effects of connectors, etc.

Presuming twisted shielded pairs or twinaxial shielded wires, the differential currents in the inner shield take a "U-turn"[13] at the discontinuous ungrounded ends, Figure 29, better described as an inductive short circuit with a voltage reflection coefficient of $\Gamma_V \geq -1$. Common mode shield currents see a capacitive open circuit, Figure 30, with voltage reflection coefficient of $\Gamma_V \leq = +1$.

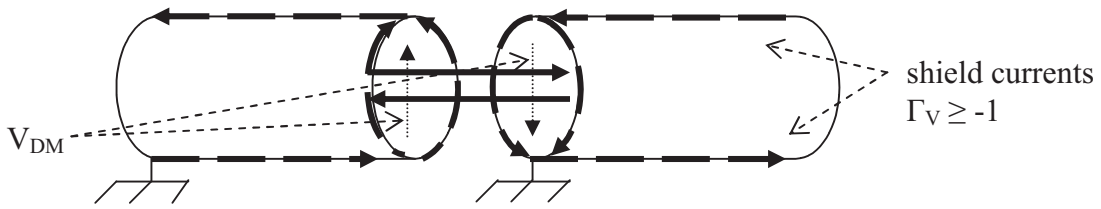

Figure 29 Differential Mode Shield Currents at Shield Gap

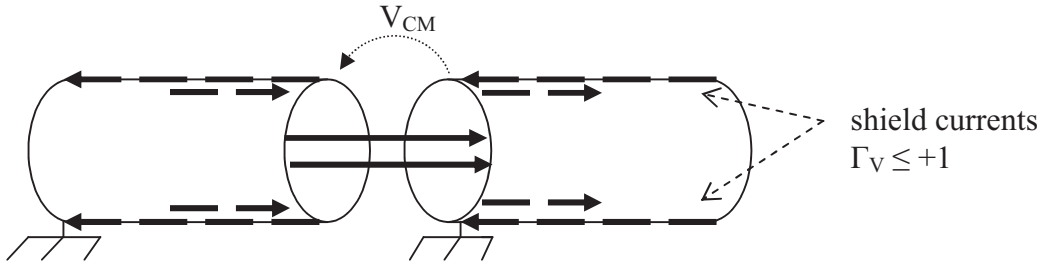

Figure 30 Common Mode Shield Currents at Shield Gap

The differential shield currents making U-turns at the open gap in the shields will induce electric fields across the pair of wires traversing the gap of about equal and opposite polarities on either side. The gap is never more than a few millimeters which is small compared to a quarter wavelength of 7.25 centimeters of, say 1GHZ signals, therefore the two oppositely polarized differential mode voltages should be of small consequence.

Common mode currents and voltages in the inner shield layer will reflect off of the open ends resulting in about twice the incident voltage at the gaps in the shield layer. Let's examine two examples, RS422 signals and Ethernet signals.

RS422 line drivers put out as much as 3 volts of common mode[14] which when reflected at the open gap in the inner shield layer will result in 6 volts across the gap assuming one side of the gap grounded and the other side open. RS422 line receivers have a common mode tolerance of ±7 volts[15] making the open gap acceptable but with little margin.

Ethernet circuits put out 1.5-2.5 peak-to-peak volts differential mode[16]. Ethernet receivers tolerate about that amount of common mode[16]. Conversion of differential mode to common mode is tightly controlled in the transmit and receive circuits, the cables, and in the connectors. Taking an Ethernet cat7 connector for example; the mode conversion, called "transverse conversion loss" (TCL) in the IEC Standards[17], is specified to be no worse than TCL(dB) = 66 – 20·log(f(MHz)) which at 1GHz is 6dB. Reflections of

twice the incident voltage or 6dB wipe out the mode conversion (TCL) of the connector making the gap in the inner shield layer a potential problem, particularly with more than one connector in the line so shielded.

Siemon experts say that we could put a single point ground (SPG) shield with a gap on one end of the foil shielded twisted pairs (FTP) shielded cat6 Ethernet cable but not the cat7 because cat6 retained the mode conversion controls in the twisted pairs.[13] Cat7 relaxed this feature because the shielding took care of the crosstalk and EMI immunity with less balance control needed in the wiring. Transformer coupling can further take care of most of the common mode problems on Ethernet and Time Triggered Gigabit Ethernet (TTGbE).

Keep in mind that this shield design is for those cables in a composite airframe exposed to the large Waveform 4 IR-drop voltages with the Waveform 5 currents on the cable shields. For those lines, both the older technology RS422[18] and 485 as well as the newer technology Ethernet[19] and TTGbE, there are now transformer and opto-isolation techniques with 1kV stand-off capability in the transformers. The transformer circuits with bifilar chokes also provide about 30-50dB of common mode isolation, more than enough to handle the 6dB spikes in the common mode voltage induced by the gap in the inner layer of shielding.

The last mitigation process for Ethernet and TTGbE systems is adaptive software whereby the line driver and/or the line receiver detect the errant signals and cancel them out at either or both ends. One or both of the line driver or line receivers are programmed to recognize the change in the signals received due to insertion loss, impedance changes, and reflections and are programmed to negate those signals to an acceptable level of bit error rate.[13] These techniques were developed when designers realized that mode conversion, crosstalk, and EMI are always present with unpredictable levels and effects, therefore the software "encryption" was designed to correct, ignore, or cancel out the errant signals caused by the EMI/EMC effects. The motivation to do so was furthered along by the problem Ethernet designers have with wire and cable shielding in that it is never maintained up to standards and, in fact, presents a safety violation when connected to two terminals operating off of two different power mains.[13]

As an aside, wire and cable shielding is more of a problem for American designers than European designers because American EEs have never come to grips with the "ground-loops" that result from shields grounded at both ends, i.e. they believe that the shield in the noise ground loop is less desirable than the circuit in the noise ground loop. EMI engineers make careers countering this errant motherhood.

CONCLUSIONS

There are three ways to reduce the lightning induced voltage IR-drop in wiring running over lengths of composite structure:

(1) The obvious – make those lengths of external skin out of aluminum or titanium, worth 40-60dB;

(2) Install a low resistance, low inductance, groundplane underneath all wire runs, worth 8-12dB, easy to do in aircraft fuselages, difficult to impossible in wings, empennages, missiles, rockets, etc.; and,

(3) Install one or two high-mu foil layers underneath the copper overbraid to shield the low frequency Waveform 5 current in the cable shield and install another layer of copper braid or foil underneath the high-mu foil ungrounded at one end, producing a transfer impedance of 10 micro-ohm per meter, peak induced voltage to peak Waveform 5 current, with no saturation. The top layer of copper braid practically ensures no saturation of the high-mu foil.
The designer must ensure that the circuits can withstand the common mode perturbation in the inner shield impedance at the ungrounded end, e.g. design in mode conversion control in the wiring and I/O circuits, transformer isolation, and/or adaptive software that detects the errant perturbation and cancels it out.

TEST PLANS

Figure 31 is a pictorial of a lab test set up for checking these theoretical models. The transfer impedance of several cable shields will be measured first as depicted in Figure 32. The plan is to perform this test with (1) a frequency sweep using a network analyzer and (2) a time domain Waveform A pulse and later, as much as possible, (3) saturate the high-mu foil shield with a Waveform 5 pulse. In order to saturate the foil, the cable shield may have to be driven directly to obtain maximum current through it. An additional test will be run on the new cables to measure the effect of the open ended shield on differential swept frequency signals.

The tests are intended to (1) demonstrate how electrical currents divide between carbon and copper and (2) verify Schelkunoff's 74 tear old theory of coaxial cable shielding.

The effects on the signals of the new layered cable shield with one end of the inner layer ungrounded will also be tested.

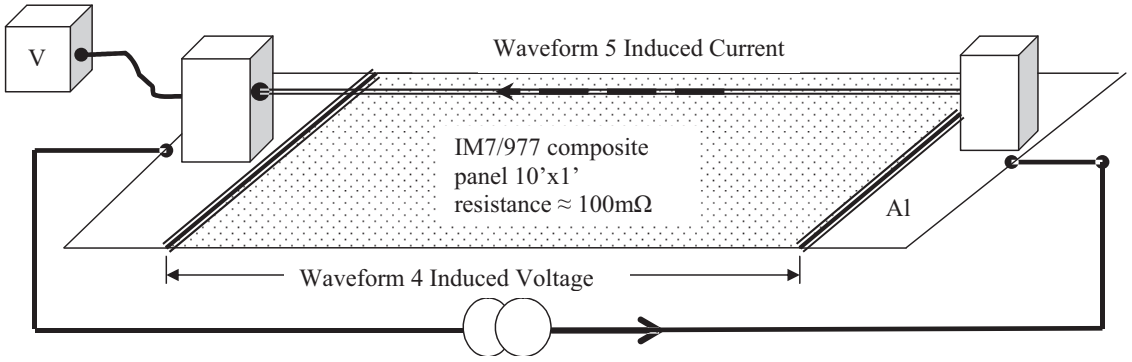

Figure 31 Indirect Lightning Test of Effect of Cable Shield on IR-Drop Induced Voltage and Waveform 5 Cable Current

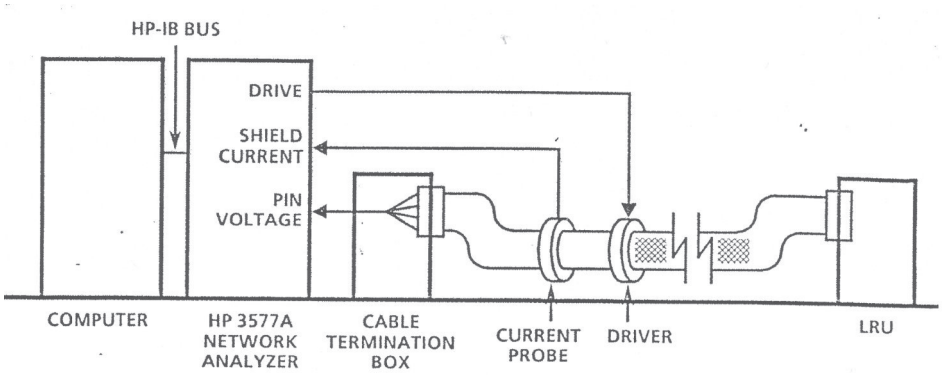

Figure 32 Cable Shield Transfer Impedance/Attenuation Test Method[11]

REFERENCES

1. Schelkunoff, S. A., "The Electromagnetic Theory of Coaxial Transmission Lines and Cylindrical Shields", The Bell System Technical Journal, Volume XIII, 1934, 532-579

2. Lee, K. S. H., Editor, *EMP Interaction: Principles, Techniques, and Reference Data*, Taylor & Francis, NY, 1995, 505-510

3. Goldman, Stanford, *Laplace Transform Theory and Electrical Transients*, Dover Publications, Inc., NY, 1966

4. SAE ARP5412A, "Aircraft Lightning Environment and Related Test Waveforms", Society of Automotive Engineers, Aerospace Recommended Practice, PA, Revised 2005-02

4. SAE ARP5415A, "User's Manual for Certification of Aircraft Electrical/Electronic Systems for the Indirect Effects of Lightning", Society of Automotive Engineers, Aerospace Recommended Practice, PA, Revised 2002-04

5. RTCA/DO-160E, "Environmental Conditions and Test Procedures for Airborne Equipment", Section 22, Lightning Induced Transient Susceptibility and Section 23, Lightning Direct Effects, RTCA Inc., DC, December 9, 2004

6. Merewether, David E., "Analysis of Shielding Characteristics of Saturable Ferromagnetic Cable Shields", IEEE Tran. EMC-12, No. 3, August 1970, 134-137 (AFRL Interaction Note 67 on www/unm.ecu.edu/summa/notes)

7. Merewether, David E., "Design of Shielded Cables using Saturable Ferromagnetic Materials", IEEE Tran. EMC-12, No. 3, August 1970, 138-141 (AFRL Interaction Note 68 on www/unm.ecu.edu/summa/notes)

8. http://raychem.tycoelectronics.com/datasheets/9-087_9-088_ElectrialShield.pdf, Catalog 1654025, Revised 12-04, Miscellaneous, "Electrical Shielding"

9. ArcelorMittal, Denise, France, www.imphy.com, brochure on Mumetal – Permphy & Superimphy, Fe-Ni Soft magnetic Alloys

10. Raychem private communication, July 2008

11. William Prather, "Cable Shield Specifications and Measurement Techniques", Aircraft EMP Standards Meeting Defense Threat Reduction Agency, Air Force Research Laboratory, Directed Energy Directorate,18 Oct 2006 [Techniques developed by Hoeft (BDM), Miller (TRW), & Prather.]

12. The Siemon Company private communication, 7/24/08, V. Maguire & D. Medeiros

13. Johnson & Graham, *High-Speed Signal Propagation*, Prentice Hall PTR, NJ, 2003

14. Texas Instruments Data Sheet, SLLS871, Nov 2007, for the AM26C31-EP Line Driver

15. Texas Instruments Data Sheet, SLLS870, Nov 2007, for the AM26C32-EP Line Receiver

16. Texas Instruments Data Sheet, SLLS428F, June 2000, Revised January 2004, TLK1501, 0.6 to 1.5 GBPS Transceiver

17. International Electrotechnical Commission Standard IEC 61076-3-104 Ed2

18. http://www.maxim-ic.com/appnotes.cfm/an_pk/2116, MAX1480A, B, Complete, Isolated RS-485/RS-422 Data Interface

19. http://www.analog.com/en/interface/digital-isolators/ADUM1200/products/product.html, ADUM1200: Dual-Channel Digital Isolator (2/0 Channel Directionality)

20. 10/100 Base-T Single Port Transformer Modules, Pulse Engineering, Inc., http://www.datasheetcatalog.org/datasheets2/19/194306_1.pdf (These have center-tapped transformers, bifilar chokes, and common mode filtering.)

21. Raychem Specification Control Drawing, EPD-RWC-21824 (courtesy of Robert Moore.)